ISSN 1330-3651 (Print), ISSN 1848-6339 (Online)
https://doi.org/10.17559/TV-20241116002134
Original scientific paper

Influence of Welding Parameters on Weld Quality and Spindle Load During Friction Stir Welding

Jozef BÁRTA*, Katarína BÁRTOVÁ, Milan MARÔNEK, František JURINA, Roman KUKUČA

Abstract: Friction stir welding brings advantage in utilisation of green joining technology even to companies dealing only with machining. In contrary to machining, FSW uses tools with not sharp geometry therefore welding parameters and tool geometry play main role in application of this process to standard machines. Different welding speed was applied during experiment to see the influence on spindle load. Results confirmed almost linear dependence between welding speed and spindle load. Highest spindle load of 2.55 kW was observed while welding 5mm thick AW7075 aluminium alloy at 800 mm/min welding speed. Experiment showed a good performance of the tool while producing good quality weld joints in welding speeds lower than 600 mm/min. Macroscopic and microscopic analysis did not show any abnormalities, however welding speeds exceeding 600 mm/min exhibited discontinuities in root section that may indicate the formation of tunnel defect. Microscopic analysis showed significant deformation of original grains in thermomechanically affected zone and very fine grain structure in stir zone.

Keywords: AW 7075-T651; friction stir welding; spindle load; structural analysis

1 INTRODUCTION

Current situation in economics as well as ecology brings forward green production technologies. Economy is pushing production into lowering the waste material and better utilisation of materials since raw materials are limited and getting higher in price every year. This is in line with ecological perspective as air pollution is worse and worse and some industrial applications are creating too much pollution in the mean of water pollution, air or soil.

Welding is a technology where pollution of the air was high and still is in some welding methods like MMAW or GMAW where a lot of fumes occur [1, 2]. Therefore, filters for vacuuming systems are getting filled quickly and need to be processed to avoid soil or water pollution. Friction stir welding is considered to be a green technology from several points of view. No particles released into the air, no light effect, full automation, are just a few of this technology benefits.

Technology is relatively young and most researchers focus on different geometry of the tool [3-7] or weldability of specific materials [8-11]. Nowadays, the FSW process is applied to materials like magnesium aluminium, copper or even steel. Moreover, some authors try to find alternative approaches to weld while using this technology. Sabari et al reported benefit of underwater FSW application in increasing the yield strength of weld joint by 20%, however the welding speed was quite low to be able to plasticise the material [12]. Some companies successfully developed the system also for additive manufacturing using friction stir welding and researchers are trying to optimise parameters and analyse the process as well as the material [13, 14].

The paper deals with the spindle load during friction stir welding as the main condition for application of technology to particular devices. Balasubramanian et al. as well as Mendelez and others were studying the forces on welding tool as a response of the material to geometry of the tool and parameters used for welding [15-18]. The resulting forces on the tool and spindle itself mostly depend on process parameters and the plasticisation level you will acquire during the process. The welding parameters can be set even for tools having complicated geometry to get sufficient material temperature and plasticisation level. Plasticisation rise with rising material temperature. The balance has to be found in order to acquire suitable weld joints with no defect. Resulting forces during the welding can seriously damage the spindle of device if the parameters of the process are not set properly. Instead of reading forces, many devices have option to read spindle load by default. This paper is focused in showing the dependence of spindle load on different welding parameters.

2 MATERIALS AND METHODS

Material used in experiment was aluminium alloy AW7075-T651 with the thickness of 5 mm. To maintain same condition, bead on plate welds were chosen instead of regular welds. This way we will prevent results distortion caused by possible differences in distance between materials to be welded. Material was welded in 'as delivered' conditions, degreased by the cleaner. To keep it in position during welding process, material was attached to the table using 4 clamps. The device used for welding and experimental setup is shown in Fig. 1. The chemical composition of the material was measured by optical emission spectroscopy and results are provided in Tab. 1.

Table 1 Measured chemical composition of AW 7075 T651 aluminium alloy (wt. %)

Al	Cr	Cu	Fe	Mg
88.7	0.178	1.740	0.201	2.511
Mn	Si	Ti	Zn	Other
0.059	0.082	0.018	6.440	0.071

To identify whether the standard milling machine is suitable for welding, the experiment was proposed. Initial task was to find out the load based on tool during welding procedure. The spindle load was observed using Dataasoft software that was getting the readings directly from the DMG Mori / DMU 85 MONOBLOCK machine, which was used for welding. Axis stroke is X 935 mm / Y 850 mm / Z 650 mm. Spindle capacity is 44 kW.

Figure 1 Milling machine DMG DMU 85 Monoblock

Self-designed tool was used for welding (Fig. 1). Probe used in this experiment was in the shape of a threaded cone cut into a regular four-sided pyramid. Probe was 4.9 mm pulled out from the shoulder. The shoulder had a triple helix-shaped groove with 0.5 mm depth. Material used for production of the 6 mm probe in diameter was tungsten carbide, whereas the shoulder with diameter of 14 mm was made of standard tool steel. There are many possibilities to influence the load with tool geometry, however that is the subject for different research task. Therefore, one tool was used with predefined welding parameters needed to be found. After obtaining a good weld the parameters window was proposed.

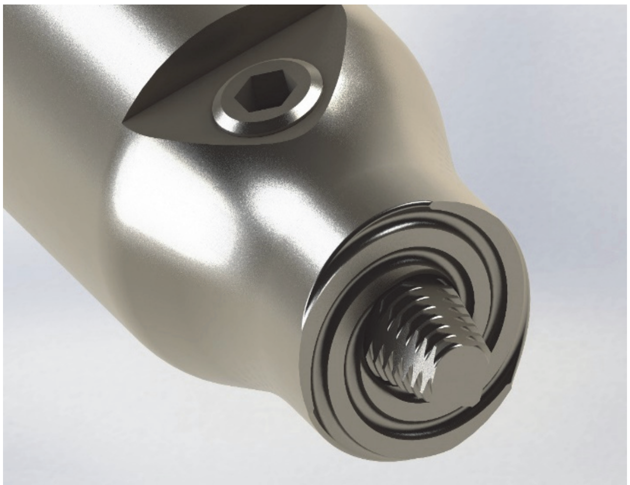

Figure 2 Self-designed welding tool

Table 2 Sample designation and parameters of welding

Sample designation	Rotational frequency of the tool / s^{-1}	Welding speed / mm/min	Shoulder immersion / mm
Sample 1	1000	300	0.2
Sample 2		400	
Sample 3		500	
Sample 4		600	
Sample 5		700	
Sample 6		800	

The parameters used for welding the aluminium are shown in Tab. 2. Parameters were constant except for welding speed. Temperature is connected to plasticisation of the material and its resistance to be stirred. Higher temperatures during welding usually occur when lower welding speed is used for welding. Welding speed above 700 mm/s did not bring satisfactory results to weld quality for this tool geometry, therefore the experiment did not continue with higher welding speeds.

Quality of weld was evaluated by computer tomograph ZEISS Metrotom 1500 and VGStudio MAX 3.0 software was used to identify porosity and other inner defects. Standard metallography was used to observe weld geometry in its cross-section. After cutting the samples, grinding and polishing was applied. Standard Kellers Reagent was used for etching and revealing the structure. Macroscopic analysis was documented using Canon camera quipped with Canon EF 100 mm macro lens.

3 RESULTS AND ACHIEVEMENTS

Welding was performed by the parameters provided in Tab. 3. Weld length was 120 mm, where its end is characteristic with the hole created by tool after leaving the material. Results show that the flash was more significant in lower welding speed. In higher welding speed the flash was lower mainly on the right side, where welding is more stable, since it is more distant from starting point where preheat is realised after immersion and hold time to plasticize the material. The discontinuity in weld width was observed in Sample 6 with welding speed of 800 mm/min. The width was narrower on the right top side, where flash was missing. On one side, it could be evaluated as a defect, however on the other side, this does not mean that the weld will show defects in the middle area.

The fact that the flash was missing in higher welding speed may point out that the tool was pushed out from material during welding process and this can influence the quality of the weld in lower section where weld root should be expected. This is caused mainly because of lower temperatures during the welding and higher material resistance to the penetration of the tool. Macrostructural analysis was realised to confirm the differences of penetration depth of the welding tool. In some cases, the non-uniformity of the weld surface was observed at the beginning of welding process which was caused by the rotation of shoulder where excessive amount of aluminium was wrapped. However, this uniformity was very shallow and after reaching stable plasticization of the material and the stable welding process, this non-uniformity was gone. This error can be avoided by lowering the waiting time after immersion of the tool, before the actual welding.

Regarding the surface state, it can be stated that the weld surface was stable, reflecting the welding speed. In lower welding speed, the weld surface texture was smoother compared to samples welded with high welding speed.

Fig. 3 shows cross-sections of each sample, where difference in root section is obvious. In low speed the material is plastic enough to mix the material up to the bottom, whereas in higher welding speeds the sharp edge from the tool rotation was observed. In samples 5 and 6 the edge is very notable and penetration in weld axis is losing. Macroscopic analysis showed the full penetration across the material thickness. Standard zones like stir zone (SZ), thermos-mechanically affected zone (TMAZ) and heat affected zone (HAZ) were observed in every weld. Significant differences on advancing side and retreating side were observed. Advancing side (left side in cross-section) showed sharp transition from stir zone to thermomechanical affected zone, whereas the retreating side (right side in cross-section) showed smooth transition. Heat affected zone was wide, showing sufficient temperature around the probe and under the shoulder.

Table 3 Weld surface appearance

Sample	Weld surface appearance
Sample 1	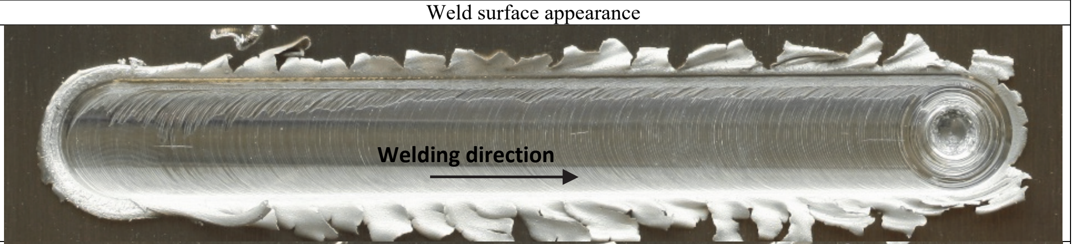
Sample 2	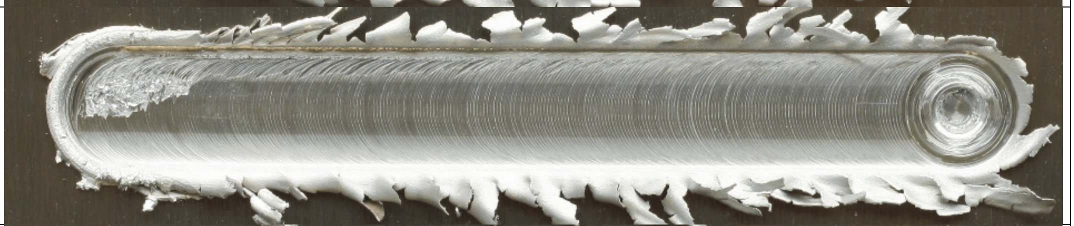
Sample 3	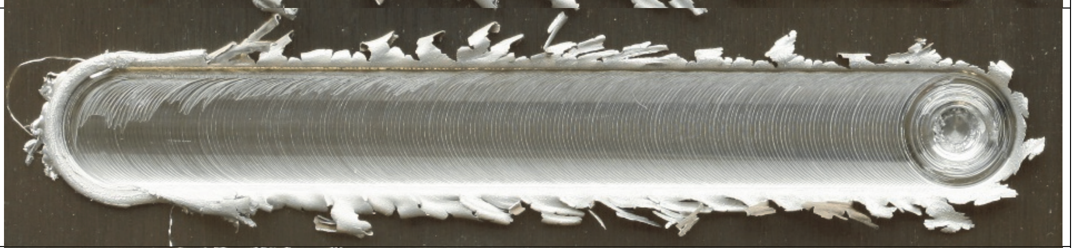
Sample 4	
Sample 5	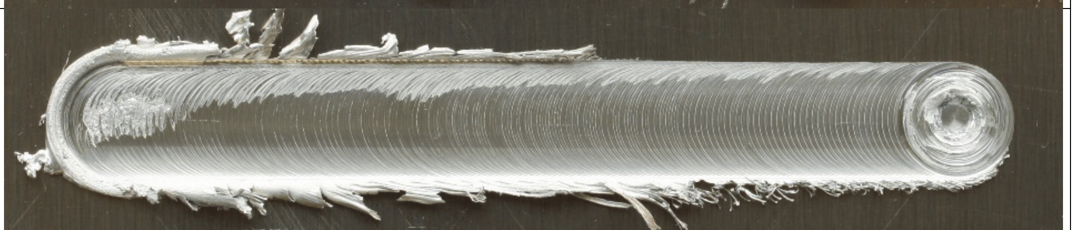
Sample 6	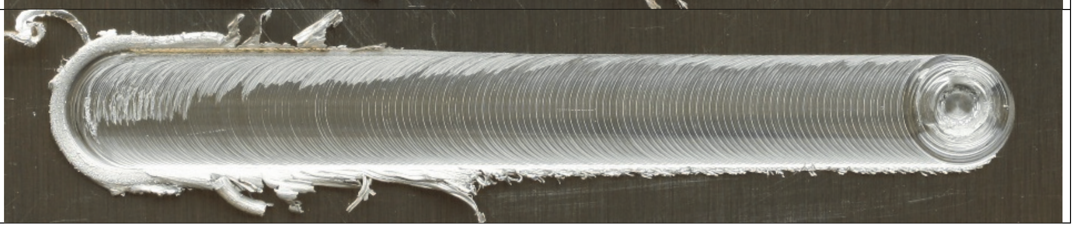

Inconsistency in penetration of the tool, shoulder specifically was observed on reinforcement of flash. Stronger reinforcement was observed in samples welded with lower welding speed.

No defects were found in all samples. Higher welding speed than 800 mm/min showed formation of tunnel defects.

Sample 5 and 6 showed voids in root section of the weld (Fig. 4). These voids had irregular shape and usually indicate formation of tunnel defect which is common mostly in weld root while using higher welding speed. This is caused by inconsistent flow of the material around the welding tool. The welding tool is pushing the material downwards, whereas plasticised material has to return upwards. If the material is not plasticized enough, tunnel defect may occur.

Microstructure was documented in all samples, however the results were very similar in all cases as expected. Therefore, only the microstructure for Sample 1 is provided.

The transition across particular zones is showed and described in Fig. 5.

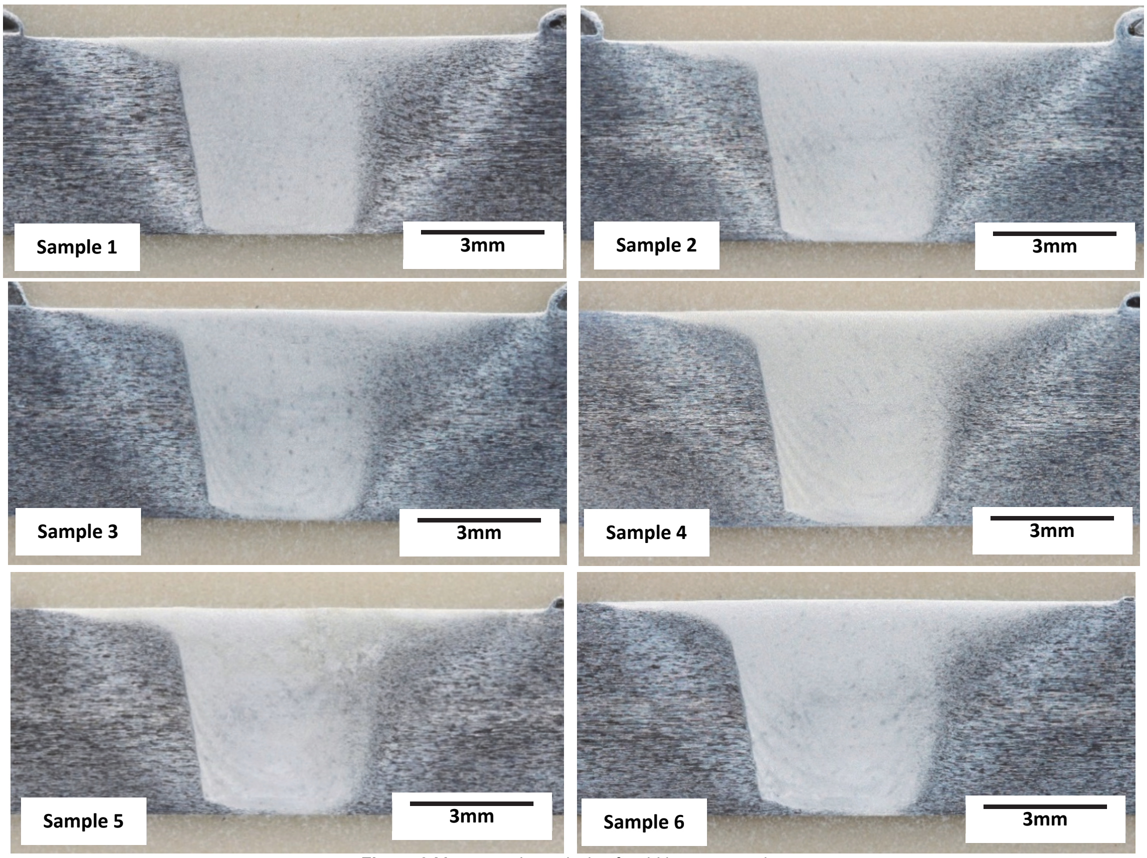

Figure 3 Macroscopic analysis of weld in cross-section

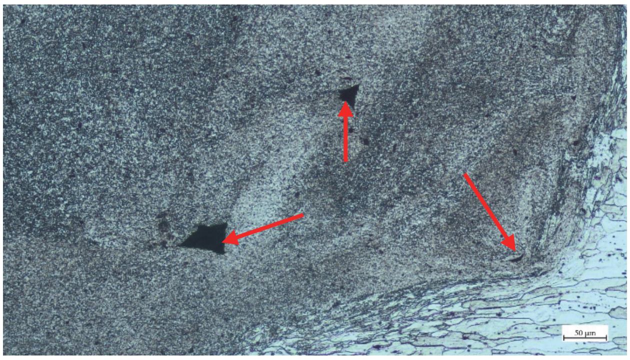

Figure 4 Voids present in Sample 6 in root section of the weld

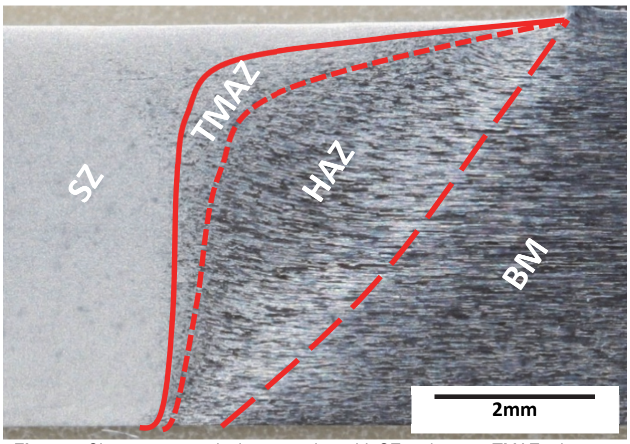

Figure 5 Close-up on particular zones in weld; SZ - stir zone, TMAZ - thermo-mechanically affected zone, HAZ - heat affected zone, BM - base material

SZ contained fine polyhedral grains with the grain size of 3 µm up to 8 µm (Fig. 6). Black particles present in microstructure we identified and carbides coming from polishing process.

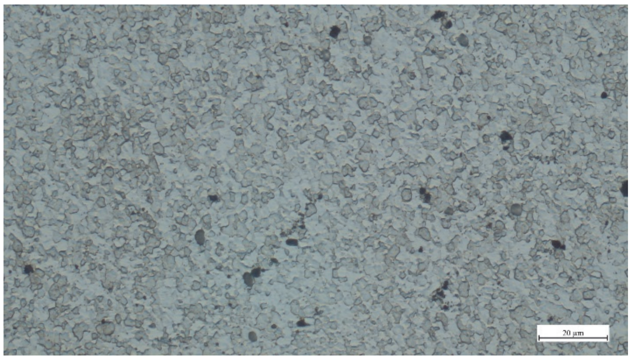

Figure 6 Microscopic analysis of weld, stir zone

Fig. 7 shows sharp transition line from SZ to TMAZ. TMAZ showed strong deformation of grains in root section of the weld heading upwards.

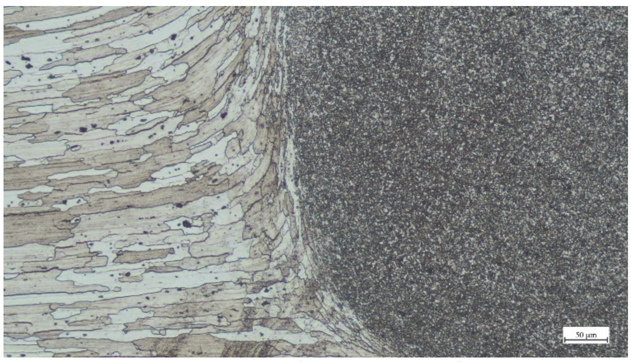

Figure 7 Microscopic analysis of weld, bottom part of advancing side

In upper section (however closer to the middle) of TMAZ, the direction of material flow was changed, heading downwards (Fig. 8). Transition from TMAZ to SZ was sharp as well.

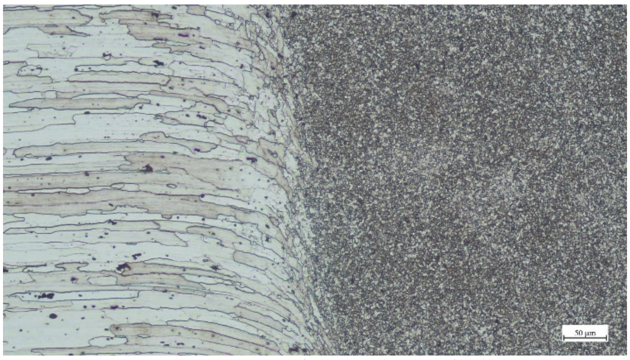

Figure 8 Microscopic analysis of weld, upper part of advancing side

Top section of advancing side was influenced by the heat origin from shoulder so there the material flow direction is not that significant as in lower sections. Transition in top section of the weld (Fig. 9) showed more fluent grain size gradient from SZ to TMAZ compared to lower sections of weld.

Figure 9 Microscopic analysis of weld, top part of advancing side

Microstructure of retreating side (Fig. 10) was characterized by gradual grain size changes in transition from SZ to TMAZ. This side does not show sharp transition compared to advancing side across the material thickness. Fig. 10 documents the transition from SZ to TMAZ in the middle part of the weld. Small deformation of original grains was observed in TMAZ.

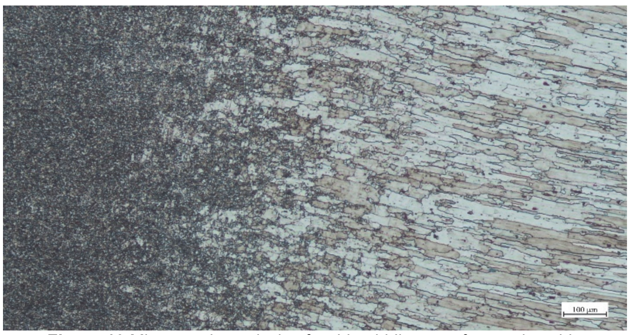

Figure 10 Microscopic analysis of weld, middle part of retreating side

Spindle load is a crucial parameter limiting the application of friction stir welding in manufacturing process. Since the high stiffness of the spindle is required for the welding process, it cannot be applied to machines having spindles with low power. Fig. 11 shows dependence of spindle load on time for every sample.

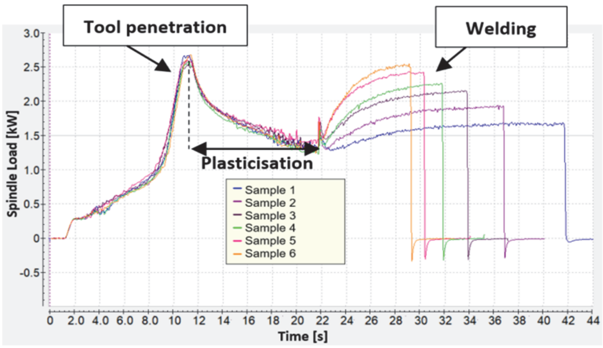

Figure 11 Spindle load during welding process

First peak of spindle power represents the penetration of the tool into the material. Subsequently, the load decreased, since 10 seconds waiting time was applied to plasticize the material before welding. Another increase of spindle load was observed during welding up to its maximum for welding process. This level was dependent on welding speed. Results showed that spindle load increased with the increase of welding speed (Fig. 12).

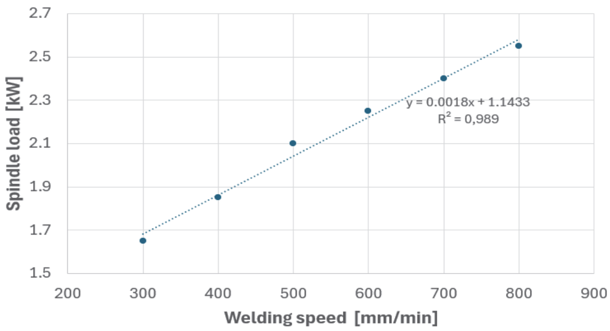

Figure 12 Spindle load dependence on welding speed

Maximum spindle load was observed during tool penetration period which was constant for every sample. Penetration speed of the tool was 20 mm/min. Lower spindle load can be reached by lowering the penetration speed.

4 CONCLUSIONS

Friction stir welding is a good option for every company having machining in their production. Moreover, possibility to use machining devices also for welding or simply switching the production process can rise their competitiveness. Following conclusions can be stated based on this research:

1. Application of the FSW technology is limited by spindle load capabilities of particular machining device.
2. Spindle load is strongly affected by the properties of material to be welded but can be influenced by welding parameters.
3. Lowest spindle load was observed in welding speed of 300 mm/min mainly due to better plasticization and thus lower resistance from base material.
4. Initial formation of tunnel defect was observed in high welding speeds (Sample 5 and 6).

5. Maximum spindle load of 2.5 kW was observed in high welding speed of 800 mm/min.
6. The dependence of spindle load on welding speed is mostly linear and higher welding speed leads to rise of spindle load.

Acknowledgement

This work was supported by the Slovak Research and Development Agency under the contract No. APVV-21-0111.

5 REFERENCES

[1] Maglić, L., Marić, D., Šolić, T., & Samardžić, I. (2022). Optimization of Synchropulsed MIG Welding Process Parameters for Welding of AW 5083 Sheets. *Materials, 15*(9), 3078. https://doi.org/10.3390/ma15093078

[2] Cortes, J. B., Philippe, S., Denis, D., Jonathan, C., Capucine, O., Naïma, El M., & Michèle, B. (2023). Biomonitoring of exposure to multiple metal components in urine, hair and nails of apprentice welders performing shielded metal arc welding (SMAW). *Environmental Research, 239*, 117361. https://doi.org/10.1016/j.envres.2023.117361

[3] Quintana, K. J. & Silveira, J. L. L. (2017). Mechanistic models and experimental analysis for the torque in FSW considering the tool geometry and the process velocities. *Journal of Manufacturing Processes, 30*, 406-417. https://doi.org/10.1016/j.jmapro.2017.09.031

[4] Radisavljevic, I. Z., Zivkovic, A. B., Grabulov, V. K., & Radovic, N. A. (2015). Influence of pin geometry on mechanical and structural properties of butt friction stir welded 2024-T351 aluminum alloy. *Hemijska industrija Chemical Industry, 69*(3), 323-330. https://doi.org/10.2298/HEMIND131206020R

[5] Anand, R. & Sridhar, V. G. (2020). Studies on process parameters and tool geometry selecting aspects of friction stir welding-A review. *Materials Today: Proceedings, Elsevier Ltd,* 576-583. https://doi.org/10.1016/j.matpr.2019.12.042

[6] Hattingh, D. G., Blignault, C., Niekerk, T. I., & James, M. N. (2008). Characterization of the influences of FSW tool geometry on welding forces and weld tensile strength using an instrumented tool. *Journal of Materials Processing Technology, 203*(1-3), 46-57. https://doi.org/10.1016/j.jmatprotec.2007.10.028

[7] Satish Kumar, P. & Shiva Chander, M. (2020). Effect of tool pin geometry on FSW dissimilar aluminum alloys - (AA5083 & AA6061). *Materials Today: Proceedings, Elsevier Ltd*, 472-477. https://doi.org/10.1016/j.matpr.2020.08.204

[8] Devaiah, D., Kishore, K., & Laxminarayana, P. (2018). Optimal FSW process parameters for dissimilar aluminium alloys (AA5083 and AA6061) Using Taguchi Technique. *Materials today proceedings, 5*(2), 4607-4614. https://doi.org/10.1016/j.matpr.2017.12.031

[9] Yuvaraj, K. P., Ashoka Varthanan, P., Haribabu, L., Madhubalan, R., & Boopathiraja, K. P. (2021).Optimization of FSW tool parameters for joining dissimilar AA7075-T651 and AA6061 aluminium alloys using Taguchi Technique. *Materials Today: Proceedings, Elsevier Ltd*, 919-925. https://doi.org/10.1016/j.matpr.2020.02.942

[10] Hussain, A. K. & Quadri, P. A. S. (2010). Evaluation of parameters of friction stir welding for aluminium AA6351 alloy. *International Journal of Engineering Science and Technology, 2*(10), 5977-5984.

[11] Dunder, M., Samardžić, I., Šimunović, G., & Konjatić, P. (2020). Steel weldability investigation by single and double-pass weld thermal cycle simulation. *International Journal of Simulation Modelling, 19*(2), 209-218. https://doi.org/10.2507/IJSIMM19-2-51

[12] Sree Sabari, S., Malarvizhi, S., & Balasubramanian, V. (2016). Characteristics of FSW and UWFSW joints of AA2519-T87 aluminium alloy: Effect of tool rotation speed. *Journal of Manufacturing Processes, 22*, 278-289. https://doi.org/10.1016/j.jmapro.2016.03.014

[13] Kumar Srivastava, A., Kumar, N., &Rai Dixit, A. (2021). Friction stir additive manufacturing – An innovative tool to enhance mechanical and microstructural properties.Materials Science and Engineering: B, 263, 114832. https://doi.org/10.1016/J.MSEB.2020.114832

[14] Singh, A. K., Bhoopendra K., Kaushal, J., Antonello, A., Antonino S., Stefania, F., & Amit, A. (2020). Friction stir welding of additively manufactured Ti-6Al-4V: Microstructure and mechanical properties. *Journal of Materials Processing Technology, 277*, 116433. https://doi.org/10.1016/J.JMATPROTEC.2019.116433

[15] Melendez, M., Tang, W., Schmidt, C., Mcclure, J. C., Nunes, A. C., & Murr, L. E. (2003). Tool Forces Developed During Friction Stir Welding. *NTRS - NASA Technical Reports Server.*

[16] Balasubramanian, N., Gattu, B., & Mishra, R. S. (2009). Process forces during friction stir welding of aluminium alloys. *Science and Technology of Welding and Joining, 14*(2), 141-145. https://doi.org/10.1179/136217108X372540

[17] Lambiase, F., Paoletti, A., & Di Ilio, A. (2018). Forces and temperature variation during friction stir welding of aluminum alloy AA6082-T6. *International Journal of Advanced Manufacturing Technology, 99*(1-4), 337-346. https://doi.org/10.1007/s00170-018-2524-6

[18] Terra, C. S. & Silveira, J. L. L. (2021). Models for FSW forces using a square pin profile tool. *Journal of Manufacturing Processes, 68*, 1395-1404. https://doi.org/10.1016/j.jmapro.2021.06.052

Contact information:

Jozef BÁRTA
(Corresponding author)
Slovak University of Technology in Bratislava,
Faculty of Materials Science and Technology in Trnava,
Institute of Production Technologies,
Paulínska 16, 91701 Trnava, Slovakia
E-mail: jozef.barta@stuba.sk

Katarína BÁRTOVÁ
Slovak University of Technology in Bratislava,
Faculty of Materials Science and Technology in Trnava,
Institute of Production Technologies,
Paulínska 16, 91701 Trnava, Slovakia
E-mail: jozef.barta@stuba.sk

Milan MARÔNEK
Slovak University of Technology in Bratislava,
Faculty of Materials Science and Technology in Trnava,
Institute of Production Technologies,
Paulínska 16, 91701 Trnava, Slovakia
E-mail: milan.maronek@stuba.sk

František JURINA
Slovak University of Technology in Bratislava,
Faculty of Materials Science and Technology in Trnava,
Institute of Production Technologies,
Paulínska 16, 91701 Trnava, Slovakia
E-mail: frantisek.jurina@stuba.sk

Roman KUKUČA
Slovak University of Technology in Bratislava,
Faculty of Materials Science and Technology in Trnava,
Institute of Production Technologies,
Paulínska 16, 91701 Trnava, Slovakia
E-mail: roman.kukuca@stuba.sk